A self-oscillating ionic polymer-metal composite bending actuator

Deivid Pugal,[1,2,a)] Kwang J. Kim,[1,b)] Andres Punning,[2] Heiki Kasemägi,[2] Maarja Kruusmaa,[2] and Alvo Aabloo[2]
[1]*Active Materials and Processing Laboratory, Mechanical Engineering Department, University of Nevada, Reno, Nevada 89557, USA*
[2]*IMS Lab, Institute of Technology, Tartu University, Tartu 50411, Estonia*

(Received 12 June 2007; accepted 4 February 2008; published online 25 April 2008)

This paper presents an electromechanical model of an ionic polymer-metal composite (IPMC) material. The modeling technique is a finite element method (FEM). An applied electric field causes the drift of counterions (e.g., Na^+), which, in turn, drags water molecules. The mass and charge imbalance inside the polymer is the main cause of the bending motion of the IPMC. The studied physical effects have been considered as time dependent and modeled with FEM. The model takes into account the mechanical properties of the Nafion polymer as well as the thin coating of the platinum electrodes and the platinum diffusion layer. The modeling of the electrochemical reactions, in connection with the self-oscillating behavior of an IPMC, is also considered. Reactions occurring on the surface of the platinum electrode, which is immersed into formaldehyde (HCHO) solution during the testing, are described using partial differential equations and also modeled using FEM. By coupling the equations with the rest of the model, we are able to simulate the self-oscillating behavior of an IPMC sheet. © *2008 American Institute of Physics*. [DOI: 10.1063/1.2903478]

I. INTRODUCTION

Electroactive polymer (EAP) based materials are valuable for many applications, from microrobotics to military and space applications. Some of the advantages of EAP materials are their light weight, noiseless actuation, simple mechanics, and large displacement capabilities. In addition, some EAPs, such as ionic polymer-metal composites (IPMCs),[1] are able to function in aqueous environments. These qualities make the materials applicable in creating artificial muscles. In this paper, we consider simulations of the IPMC type materials using the finite element method (FEM).

IPMC materials are highly porous polymer materials, such as Nafion™, and are filled with an ion-conductive liquid. Some IPMCs are water based, operating in an aquatic environment where the current is caused by ions such as Na(+) and K(+) being dissociated in water. Another kind of IPMCs—ionic liquid based—does not need a wet environment to function. A sheet of an ionic polymer is coated with a thin metal layer, usually platinum or gold. All free, mobile cations inside the polymer migrate towards an electrode due to an applied electric field, causing an expansion of the material on one side of the sheet and contraction on the other side, resulting in the bending of the sheet.

In order to simulate the actuation of an IPMC sheet, we need to solve coupled problems, which will be difficult due to the complex nature of the bending. The simulations take place in different domains such as mechanical, electrostatic and mass transfer, and even electrochemical for more advanced models. Some authors[2,3] have already simulated mass transfer and electrostatic effects, and we used similar approaches in our model. Toi and Kang showed a FEM including the viscosity terms during the transportation processes.[4] The basis of this described model is a rectangular beam with two pairs of electrodes. Our approach to simulating mechanical bending is to take advantage of the numerical nature of FEM problems—to use continuum mechanics equations instead of the more commonly used analytical equations.[5,6] By coupling equations from different domains, we get a model of an IPMC muscle sheet, which allows us to use it as a starting point for solving more complex problems; thus, we have introduced a simulation of electrochemical reactions using a platinum electrode of an IPMC sheet, leading to a self-oscillating actuation. Spontaneous oscillations are common phenomena in nature, including electrochemical systems such as oxidation of organic materials and metals.[7] Under certain conditions, such systems can generate oscillations.[8] We have conducted a series of tests, where an IPMC sheet has been immersed into an acidic formaldehyde (HCHO) solution and exposed to a constant potential. The measurements, however, show current oscillations, which, in turn, result in an oscillating bending of the IPMC sheet.[9] Hence, we have introduced a FEM model in this paper to describe the time-dependent bending of a self-oscillating IPMC.

II. BENDING SIMULATION DETAILS

An IPMC sheet consists of a polymer host and a metal coating. In our experiments, we used Nafion™ 117 that was coated with a thin layer of platinum. Mass transfer and electrostatic simulations were performed in three mechanical domains—pure backbone polymer, pure platinum coating, and a mixture of polymer and platinum. Some platinum diffuse into the polymer host during the coating process.[10] The physical properties and dimensions of a pure 2-μm-thick platinum coating are considered only when calculating the

a)Electronic mail: david@ut.ee.
b)Electronic mail: kwangkim@unr.edu.

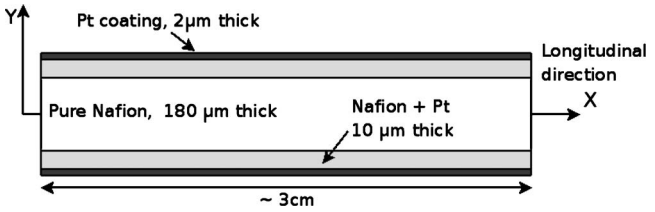

FIG. 1. Illustration of domains and dimensions used in simulations. The length of 3 cm was used also in a number of experiments. Note that there are three different mechanical domains—pure Nafion™ polymer, pure Pt coating, and a diffusion layer where Pt has diffused into the polymer.

bending. These tests give us five mechanical domains as shown in Fig. 1. Most simulations are carried out on an IPMC strip, 2–4 cm long, with a 200-μm-thick polymer, including a 10-μm-thick Pt diffusion region on each side, and coated with 2-μm-thick platinum, in a cantilever configuration. One end of the strip is fixed.

The Nernst–Planck equation describes diffusion, convection, and, in the presence of an electric field and charges, migration of the particles. The general form of the equation is

$$\frac{\partial C}{\partial t} + \nabla(-D\nabla C - z\mu FC\nabla\Phi) = -\mathbf{u}\cdot\nabla C, \tag{1}$$

where C is the concentration, D the diffusion constant, F the Faraday constant, $\mathbf{u}$ the velocity, z the charge number, ϕ the electric potential, and μ the mobility of species. The mobility of the species is found using the known relation $\mu=D/RT$, where T is the absolute temperature and R is the universal gas constant. Movable counterions are described by Eq. (1). As the anions are fixed, they maintain a constant charge density throughout the polymer. After a voltage is applied to the electrodes of an IPMC, all free cations start migrating towards the cathode, causing a current in the outer electric circuit. Due to the fact that ions cannot move beyond the boundary of the polymer, charges start accumulating, resulting in an increase in the electric field, which cancels out the applied field. The process could be described by Gauss law as follows:

$$\nabla\cdot\mathbf{E} = -\Delta\Phi = \frac{F\cdot\rho_c}{\varepsilon}, \tag{2}$$

where ρ_c is the charge density, c is the absolute dielectric constant, and E is the strength of the electric field. The charge density variable is related to charge concentration as follows:

$$\rho_c = zC + z_{\text{anion}}C_{\text{anion}}. \tag{3}$$

The second term in Eq. (3) is constant at every point of the polymer. The coupling between Eqs. (1) and (2) is strong, i.e., no weak constraints were used. The absolute dielectric constant ε could be explicitly written as $\varepsilon=\varepsilon_0\varepsilon_r$, where ε_0 is the dielectric constant in vacuum and is equal to 8.85×10^{-12} F/m. The measured value of the absolute dielectric constant ε is shown in Table I. A steady state of the cations forms when the electric field, created by distribution of cations, cancels out the applied electric field. The strength of the electric field inside the polymer is approximately zero, as

TABLE I. Parameter values used in bending simulations.

Parameter	Value	Unit
D	1×10^{-5}	cm^2/s
R	8.31	l/(K mol)
T	293	K
z	1	...
F	96.5×10^6	mC/mol
ϵ	25	mF/m
G	110	K m/mol
H	10	$N\,m^4/mol^2$
α_{polymer}	0	s^{-1}
β_{polymer}	1.5	s

shown in Fig. 2. The steady state cation concentration, with the average value of 1200 mol/m^3, is also shown in the same figure. It is interesting to note that there are fluctuations in charge distribution only in thin boundary layers, leading to the conclusion that there is no charge imbalance inside the polymer. The general understanding is that the locally generated charge imbalance near the platinum electrodes is directly connected to—and mainly responsible for—the bending of an IPMC.[11] Therefore, we define the longitudinal force per unit area at each point in the polymer of an IPMC as follows:[6]

$$\mathbf{F} = (G\rho_c + H\rho_c^2)\hat{x}, \tag{4}$$

where ρ_z is the charge density, and G and H are constants found by fitting simulations, according to experimental results, using system identification. The values of the constants are shown in Table I, and it is interesting to note that the ratio of G/H is the value suggested by Wallmersperger *et al.*[6] Equations (1)–(4) are described only for the pure Nafion™ and Pt diffusion domain (see Fig. 1). There is neither ion diffusion nor migration in the thin Pt coating domain.

To relate the force in Eq. (4) to the physical bending of an IPMC sheet, we introduce a set of continuum mechanics equations that are effective in all domains (Fig. 1). These

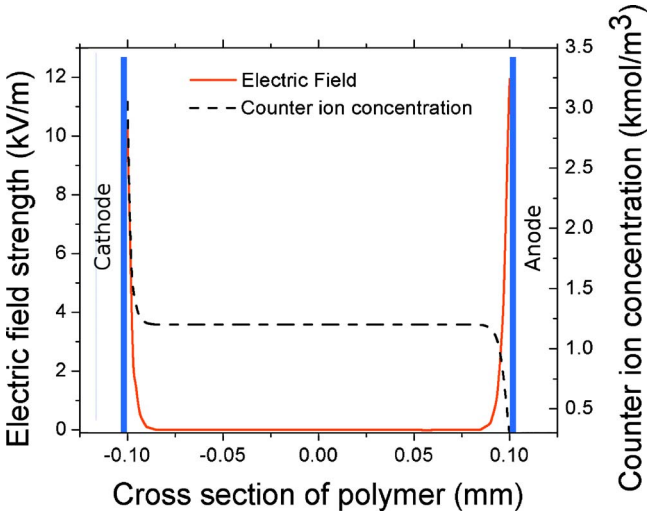

FIG. 2. (Color online) The concentration of counterions and the electric field strength inside the polymer according to simulations for a potential of 2 V.

TABLE II. Material parameters used in continuum mechanics equations.

Parameter	Value	Unit	Domain where applied
E_x	200	MPa	Nafion™
ν_N	0.49	⋯	Nafion™
E_{Pt}	168	GPa	Pt
ν_{Pt}	0.38	⋯	Pt
E_{diff}	84	Gpa	Pt diffusion layer (estimated)
ν_{diff}	0.42	⋯	Pt diffusion layer (estimated)

equations are described in the COMSOL MULTIPHYSICS structural mechanics software package. Normal and shear strains are defined as

$$\varepsilon_i = \frac{\partial u_i}{\partial x_i}, \quad \varepsilon_{ij} = \frac{1}{2}\left(\frac{\partial u_i}{\partial x_j} + \frac{\partial u_j}{\partial x_i}\right), \tag{5}$$

where u is the displacement vector, x denotes a coordinate, and indices i and j range from 1 to 3 and denote components in the x, y, or z direction correspondingly. The stress-strain relationship is

$$\sigma = D\varepsilon, \tag{6}$$

where D is a 6×6 elasticity matrix, consisting of the components of Young's modulus and Poisson's ratio. The system is in equilibrium if the relation

$$-\nabla\cdot\sigma = \mathbf{F} \tag{7}$$

is satisfied. This is Navier's equation for displacement. The values of Young's modulus and Poisson's ratios, which are used in the simulations, are shown in Table II. The values for the platinum diffusion region are not measured but, instead, estimated as an average of values of the pure Nafion™ and Pt region.

As our simulations are dynamic rather than static, we have to introduce an equation to describe the motion of an IPMC sheet. To do that, we use Newton's second law as follows:

$$\rho\frac{\partial^2\mathbf{u}}{\partial t^2} - \nabla\cdot c\,\nabla\mathbf{u} = \mathbf{F}, \tag{8}$$

where the second term is Navier's static equation and c is Navier's constant for a static Navier equation. The first term in Eq. (8) introduces the dynamic part of the problem. Several authors have reached the conclusion that IPMC materials exhibit viscoelastic behavior,[12,13] which is especially noticeable during high frequency movements.[14] However, we include the viscoelastic term in our equations by means of the Rayleigh damping[15] model, which is described for a one-degree-of-freedom system as follows:

$$m\frac{d^2u}{dt^2} + \xi\frac{du}{dt} + ku = f(t), \tag{9}$$

where the damping parameter ξ is expressed as $\xi=\alpha m-\beta k$. The parameter m is mass, k is stiffness, and α and β are the correspond damping coefficients. The equation for the multiple degrees of freedom is

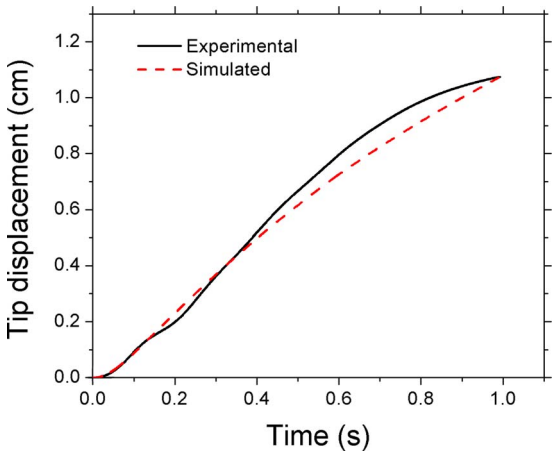

FIG. 3. (Color online) Experimental and simulation results of tip displacement. The simulation is done for a potential of 2 V. Although there is a slight difference in graphs in the large displacement region, the model gives a precise estimation for smaller displacement.

$$\rho\frac{\partial^2\mathbf{u}}{\partial t^2} - \nabla\cdot\left[c\,\nabla\mathbf{u} + c\beta\,\nabla\frac{\partial\mathbf{u}}{\partial t}\right] + \alpha\rho\frac{\partial\mathbf{u}}{\partial t} = \mathbf{F}. \tag{10}$$

By coupling Eq. (10) with the previous equations, a good basic model for the IPMC actuation has been obtained. The damping equation is very necessary to accurately describe the movement of an IPMC strip. Although the values of the parameters α and β are empirical (see Table I), they have an important role in improving the dynamical behavior of the model for nonconstant applied voltages.

All of the values used in the simulations are specified in Tables I and II. Figure 3 shows a comparison between the simulation and an actual experiment.[16] Additional comparative figures are introduced in the next section.

MODELING SELF-OSCILLATIONS

We have conducted a series of tests with IPMCs with a constant electric field in formaldehyde (HCHO) solution. Measurements show that the current oscillations begin from an applied potential of about 0.75 l. More information about the experiments and their conclusions are described in a previous paper.[9] The studies demonstrate that there are sequential electrochemical reactions taking place on the platinum cathode. The initial burst of the current is caused by the reaction

$$\mathrm{CO_{ads}} + \mathrm{OH_{ads}} \rightarrow \mathrm{CO_2} + \mathrm{H^+} + e^- + 2*, \tag{11}$$

where the subscript ads denotes species adsorbed on the platinum and $\cdot$ denotes an active platinum site. The result of reaction (11) is the clearing up of two platinum sites, which causes co to adsorb again. Chronopotentiometry scans show that before reaction (11), the following reactions occur:

$$\mathrm{HCHO} + * \rightarrow \mathrm{Pt\text{-}CHO_{ads}} + \mathrm{H^+} + e^-, \tag{12}$$

$$\mathrm{Pt\text{-}CHO} \rightarrow \mathrm{Pt\text{-}CO_{ads}} + \mathrm{H^+} + e^-, \tag{13}$$

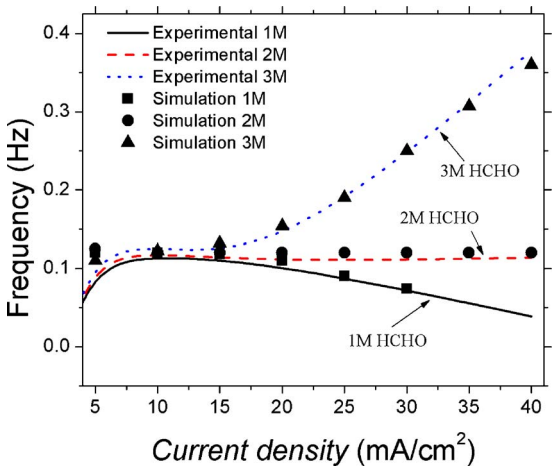

FIG. 4. (Color online) Experimental and simulated frequency dependence on the concentration of HCHO and the applied current density. Simulations for 1*M* HCHO concentration do not go past 30 mA/cm^2, because the given equation system did not give reasonable results beyond that current density.

$$H_2O + * \leftrightarrow \text{Pt-OH}_{ads} + H^+ + e^-, \tag{14}$$

HCHO is dissociated on the electrode surface at lower anodic potentials. Higher anodic potentials cause dehydrogenation of the water, resulting in water oxidation with an intermediate Pt-OH formation. We believe that these reactions lead to oscillating potentials, which, in turn, lead to the self-oscillating motion of the IPMC sheet.

A series of chronopotentiometry scans was conducted to characterize the oscillations for different HCHO concentrations and their current densities. As was discussed in our previous paper,[9] the oscillations start at approximately 7 mA/cm^2. The experiments were conducted up to the current density values of 40 mA/cm^2. Tests with HCHO concentrations of 1*M*, 2*M*, and 3*M* show that oscillation frequencies remain constant up to the current density of 14 mA/cm^2. When current is increased further in 1*M* HCHO, the frequency decreases; in 2*M* HCHO, the frequency remains constant. In the 3*M* HCHO solution, the frequency starts to increase, as shown in Fig. 4. Our goal is to develop a model to decribe the frequency behavior that is dependent on the HCHO concentration and the current density. The basic model and concepts are introduced by Kim[17] and Strasser *et al.*[18] To describe the oscillations, four dynamic parameters and, therefore, four differential equations must be observed: the concentrations of adsorbed OH and CO, the change of the double layer potential due to electrochemical reactions, and the change of the concentration of HCHO near the surface of platinum. First, two variables are expressed for a certain current density and HCHO concentration as follows:[17]

$$\dot{\theta}_{CO} = k_2 M - k_4 \theta_{CO} \theta_{OH}, \tag{15}$$

$$\dot{\theta}_{OH} = k_3 \theta_{CO} M - k_{-3} \theta_{OH} - k_4 \theta_{CO} \theta_{OH}, \tag{16}$$

where θ_{CO} and θ_{OH} are the normalized adsorption coverages of CO and OH. Variables k and M are described by the following equations:

$$k_i(\phi) = \exp[s_i(\phi - \phi_i)], \tag{17}$$

$$M = (1 - \theta_{CO} - \theta_{OH}), \tag{18}$$

where s_z are modeling coefficients and ϕ_z are potentials of the reactions.[17] The highly dynamic model introduces the double layer with thickness δ near the platinum electrode. At the far end of the layer, the concentration of the formic acid is considered constant and, due to the adsorption of HCHO on Pt, the concentration of the solution changes near the electrode. There are two components responsible for the decrease in the concentration. The first one is the direct oxidation of the formic acid to CO_2 and $2H^{\phi}$; the second one is the adsorption of CO on the platinum surface due to electrochemical reactions.[18] The mechanism that restores the HCHO concentration near the surface is diffusion. The amount of the formic acid decreases significantly when the adsorption rate is high and increases due to the diffusion during the low adsorption period. The equation describing the diffusion process is

$$\frac{\partial c_{FA}}{\partial t} = \nabla \cdot (D_{FA} \nabla c_{FA}), \tag{19}$$

with a constant concentration at the far end of the double layer and flux

$$f = k_2 M (1 + k c_r) S_{tot} \tag{20}$$

as a boundary condition on the electrode. Here, S_{tot} denotes the total number of the platinum sites per surface area. ζ_r is the normalized concentration near the boundary layer and is equal to $\zeta_r = c_{FA}/C_O$, where C_O is the initial concentration. The variable k is a simulation constant. The second term in Eq. (20) represents a simplified version of the direct oxidation path.[18] By considering these equations and the interesting nature of the frequency characteristic for different concentrations of HCHO (Fig. 4), we can now describe the empirical gray box[19] equation for the last dynamic variable—the double layer potential-as follows:

$$\dot{\phi} = \frac{1}{c_{dl}}[j_{th} - j_d + ABj^2(-j - j_{th})c_r - S_{tot}F(k_1 M + k_4 \theta_{CO}\theta_{OH})], \tag{21}$$

where j is the applied current density, j_{th} is the threshold current density with an approximate value of 10 mA/cm^2, and j_d is the direct current density and is proportional to the second term in Eq. (20). The variable B is explicitly written as $B = c_o - c_{natural}$, where $c_{natural}$ corresponds to a concentration of 2*M*. This is denoted as a "natural" concentration, as shown in Fig. 4. The oscillation frequency for the case $c_o = c_{natural} = 2M$ does not depend on the applied current density. The numeric data can be found in Table III. The third term in Eq. (21) is empirical and reflects the intriguing behavior of the oscillation frequencies for the different formic acid concentrations. Other terms are similar to the ones described by Strasser *et al.*:[18] however, some values are adjusted to get realistic simulation results. The comparison of the measured voltage oscillation with the simulation data can be seen in Fig. 5. The simulation does not require any change in the boundary or initial conditions of the basic model, which is described in the previous section. Equations (15)–(17) and

TABLE III. Variables and values used in the simulation of electrochemical oscillations.

Parameter	Value	Unit
S_{tot}	0.5×10^{-5}	mol/cm^2
C_{dl}	1	mF/cm^2
A	1.2	cm^7/(mA^2 mol)
k	100	⋯
ε[a]	2×10^{-2}	cm
D_{Fa}[a]	2.5×10^{-5}	cm^2/s
$\phi_{1,2,3-3,4}$[b]	[0.2, 0.3, 0.01, 0.512, 0.77]	V
$S_{1,2,3-3,4}$[b]	[10, −11, 9, −9, 20]	V^{-1}

[a]Reference 18.
[b]Reference 17.

(21) are simulated using the weak form of the differential equation on the anode boundary.

By using the obtained voltage output in the base FEM, described in the previous section, one can simulate the oscillating deflection of an IPMC muscle. Two sample results for the different HCHO concentrations and current densities are shown in Figs. 6 and 7. As can be seen, the amplitude, frequency, and, for the most part, the shape of the deflection show a reasonable agreement between the modeling and the experimental data. There is disharmony at the areas of maximum deflection. The experiments show distinctly sharp deflections in comparison to the smoother simulation results.

SUMMARY AND CONCLUSIONS

We have developed a FEM to simulate the actuation of an IPMC. The model is largely based on physical quantities and well known or measurable variables. The migration and diffusion of the counterions inside the Nafion™ polymer are described by using the electric field change caused by the charge imbalance. This, in turn, is coupled with continuum mechanics and dynamics equations, forming a complete system of equations to describe the bending of an IPMC sheet.

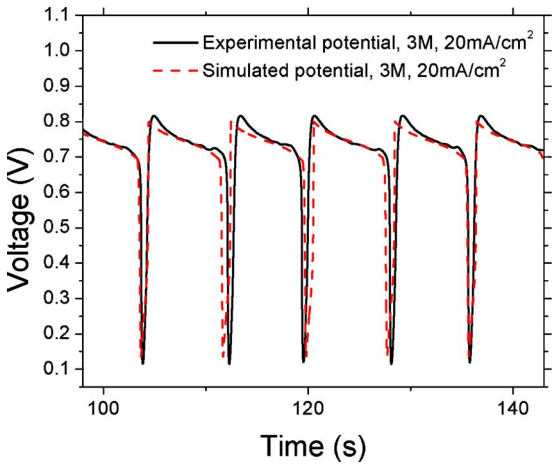

FIG. 5. (Color online) Potential oscillations. Measured data (Ref. 17) and simulated data for the 3*M* HCHO solution. The potential oscillations were measured between the cathode and anode of the IPMC strip during the experiment. The applied current was maintained at a constant value of 20 mA/cm^2.

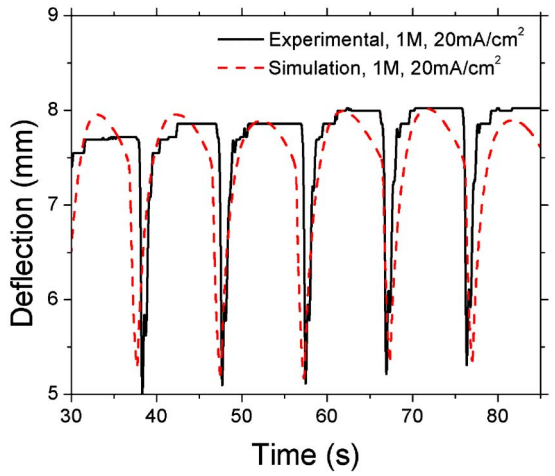

FIG. 6. (Color online) Oscillating tip displacement. Experimental (Ref. 17) data and simulation data for 1*M* HCHO solution and an applied current density of 20 mA/cm^2.

The comparison of the experimental and simulated tip displacements in time shows reasonable agreement, especially in smaller deflections. Future work will include more precise simulations for large displacements, possibly including equations that describe the voltage distribution on the surface of the electrodes that are dependent on the curvature of the IPMC. Observing the surrounding environment of the IPMC could be a factor in the next series of experiments.

The second part of the work describes the extended model for self-oscillating IPMCs. The oscillations occur when a platinum-coated IPMC is immersed into HCHO containing solutions and subjected to a constant potential or current. The extended model takes into account the changes in the HCHO concentration as it nears the electrode and the poisoning level of the platinum sites. This, in turn, results in the oscillating double layer potential, which is used in the base model to calculate the time-dependent tip displacement of the IPMC muscle. Most of the time, the model follows the simulation data closely. The experimental deflection demonstrated distinctly sharp movements at certain regions, but the

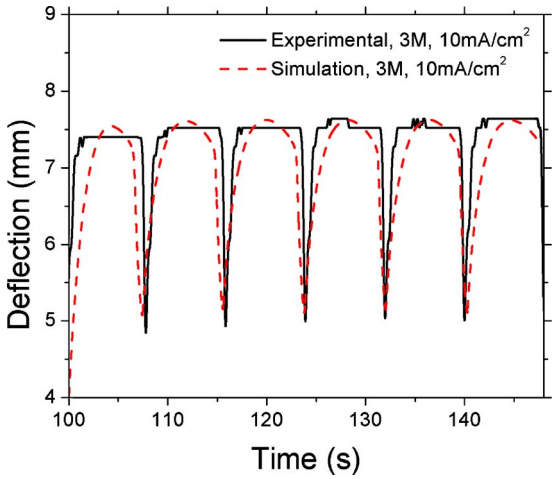

FIG. 7. (Color online) Oscillating tip displacement. Experimental (Ref. 17) data and simulation data for 3*M* HCHO solution and an applied current density of 10 mA/cm^2.

simulation gives smoother displacement profiles. Future work will include further studies on this interesting behavior in order to improve the model.

ACKNOWLEDGMENTS

We want to acknowledge the support of the US Office of Naval Research (N00014-04-0673) and Estonian Science Foundation Grant Nos. 6763 and 6765. Also we acknowledge the Estonian Archimedes Foundation for travel support of D.P. to the University of Nevada, Reno.

[1]M. Shahinpoor and K. J. Kim, Smart Mater. Struct. **10**, 819 (2001).
[2]T. Wallmersperger, B. Kroplin, and R. W. Gulch, Mech. Mater. **36**, 411 (2004).
[3]S. Nemat-Nasser and S. Zamani, J. Appl. Phys. **100**, 064310 (2006).
[4]Y. Toi and S.-S. Kang, Comput. Struct. **83**, 2573 (2005).
[5]S. Lee, H. C. Park, and K. J. Kim, Smart Mater. Struct. **14**, 1363 (2005).
[6]T. Wallmersperger, D. J. Leo, and C. S. Kothera, J. Appl. Phys. **101**, 024912 (2007).
[7]B. Miller and A. Chen, J. Electroanal. Chem. **588**, 314 (2006).
[8]K. Krischer, J. Electroanal. Chem. **501**, 1 (2001).
[9]D. Kim, K. J. Kim, Y. Tak, D. Pugal, and I.-S. Park, Appl. Phys. Lett. **90**, 184104 (2007).
[10]S. Nemat-Nasser and Y. Wu, J. Appl. Phys. **93**, 5255 (2003).
[11]S. Nemat-Nasser and J. Y. Li, J. Appl. Phys. **87**, 3321 (2000).
[12]K. M. Newbury and D. J. Leo, J. Intell. Mater. Syst. Struct. **14**, 333 (2003).
[13]K. Yagasaki and H. Tamagawa, Phys. Rev. E **70**, 052801 (2004).
[14]K. M. Newbury and D. J. Leo, J. Intell. Mater. Syst. Struct. **14**, 343 (2003).
[15]J. W. S. Rayleigh, *The Theory of Sound* (Dover, New York, 1945), Vol. 2, p. 226.
[16]A. Punning, M. Kruusmaa, and A. Aabloo, Sens. Actuators, A **133**, 200 (2007).
[17]D. Kim, Ph.D. thesis, University of Nevada, Reno, 2006.
[18]P. Strasser, M. Eiswirth, and G. Ertl, J. Chem. Phys. **107**, 991 (1997).
[19]M. Shahinpoor and K. J. Kim, Smart Mater. Struct. **13**, 1362 (2004).